DEVELOPMENT OF A SOLAR WATER HEATER

Engr. Dauda R.M., Prof. Pam G.Y., Dr. Anafi F.O.

Abstract— A double – glazed thermosyphon solar water heater was designed and optimised. This was based on weather data for Zaria, Nigeria (latitude 11.12 °N and longitude 7.8 °E), hot water storage capacity of 0.1m^3 and desired water outlet temperature of 70^oC. The geometric parameters optimised via a parametric study air – gap spacings, L_1,L_2, collector tube internal diameter, d_i and absorber plate thickness, δ in order to reduce thermal losses, enhance heat gained by the water and ensure reduced cost of the system. A model of the system was developed based on the values of the system characteristics, component sizes obtained from the design calculations and parametric study, which was used for the simulation of the system performance using the Transient System Simulation (TRNSYS 16) software. The system was constructed and then tested experimentally for three (3) days. Results showed that the simulation carried out was (1) 96.56%, 97.63% and 97.49% accurate for the 3 days, for the storage tank inlet temperatures; (2) 95.28%, 93.35% and 94.26% accurate for the 3 days, for the collector inlet temperatures. The average daily simulated/experimented efficiencies for the 3 days were 60%/ 58%, 59%/ 56% and 56%/ 53% respectively. This difference in performance was largely attributed to the fact that the data used for the simulation were strictly based on assumptions while the actual/measured data were used for the experiments.

Index Terms— Absober Plate thickness, Air-gap space, Heat Removal Factor, Insulation Thickness, Storage Tank Temperature, Top heat loss coefficient, TRNSYS

1.0 INTRODUCTION

Energy resources are classified into two types: renewable resources (R.R.) including solar energy, wind power, hydraulic energy, geothermal energy and biomass energy, and non-renewable resources (N.R.R) that cannot be replenished; such as crude oil, nuclear energy, coal and natural gas. According to British Petroleum [1], power generated from renewable resources has increased to 14 % of the total growth in global power generation [2]. However, because of the enormous growth in the energy consumption, this growth is not enough to reduce the level of carbon emissions and to meet the Millennium Development Goals (MDGs) by the year 2030 [2]. Today, most of the commercial and industrial hot water demands in Nigeria are met mainly by burning wood or using electric water heaters. Unfortunately, the rising energy cost, environmental concerns, and the depleting nature of the current primary energy sources in use have made burning of wood and the use of electric water heaters less attractive. However, utilizing solar water heaters for domestic or commercial purposes such as in hotels, restaurants, hospitals and especially in rural areas, will help achieve the Millennium Development Goals (MDGs) of reducing carbon emissions by the year 2030 since the use of the solar water heaters will significantly reduce the cost of energy consumption and it requires little maintenance in the long run. Furthermore, the world's population is expected to increase to 8.1 billion by 2030 and hence, the average carbon emissions cap for each individual must be reduced to about 3.7 tCO2/year to achieve the Millennium Development Goals by 2030. Therefore, carbon emissions must be reduced, and this can be achieved by reducing power consumption and/or increasing the percentage of the energy generated by using clean resources like solar, wind, geothermal and hydro energy.

[3] investigated the effect of the air gap spacing of double glassed doors in closed refrigerated vertical display cabinets. The results showed that when the size of the air gap was very small (about 5 mm), the heat transfer was mainly due to conduction: as the gap spacing increased, air began to move due to natural convection which led to an increase in the convective heat loss. Therefore, the sizes of the top and lower air gap spacing have an effect on the amount of heat loss from the system.

[4] conducted a parametric study in an indirect heating integrated solar water heater with double glass cover, in order to minimize heat losses. The air gap spacing between the absorber and the inner glass cover (L_1) and between the two glass covers (L_2) for the system with 0.7 m x 1.35 m absorber area were varied within the range of 15-50 mm to investigate which combination of gap sizes (L_1, L_2) would result in minimum total heat losses, including radiation and convection losses. The results showed that a combination of air gaps L_1 and L_2 of 40 mm and 25 mm were obtained as optimum values. These values are yet to be experimentally determined.

[5] designed, simulated and constructed a thermosyphon solar water heater in which the effect and sensitivity of varying collector tube centre to centre distance, absorber plate thickness, number of glass covers and collector tilt angle were studied on the heat removal factor. The results of the simulation revealed that the thermosyphon solar water heater with collector area of 2.24 m^2 was capable of supplying a daily domestic water of 0.1 m^3 at temperatures ranging from 56 ℃ for the worst month (August) to 81 ℃ for the best month (April).

This study investigated and numerically determined the optimum size of air gaps (L_1 and L_2) in the solar water heater,

with the view of minimising heat losses associated with collector surface and increasing the heat gained by the water.

2.0 DESCRPTION OF DOUBLE-GLAZED SOLAR WATER HEATER

The solar water heater is comprised of an absorber plate, glazing (glass covers), storage tank, frame/stand and fluid passage/connecting pipes as shown in Figure 1. The storage tank is made up of two compartments (the inner and outer tanks) separated by 50 mm thick insulation wall made of fibre glass wool. The collector assembly housed the absorber plate, fluid passage tubes (risers and headers) and the glazing. A series of riser tubes connected to upper and lower headers (all made up of copper) were attached to the absorber plate. The upper header connects to the inlet of the storage tank, while the lower header connects to the outlet of the storage tank. The frame, which holds the storage tank and the collector assembly together was made of hard afara wood. Flexible UPVC Tigre pipes connect the storage tank and the collector assembly.

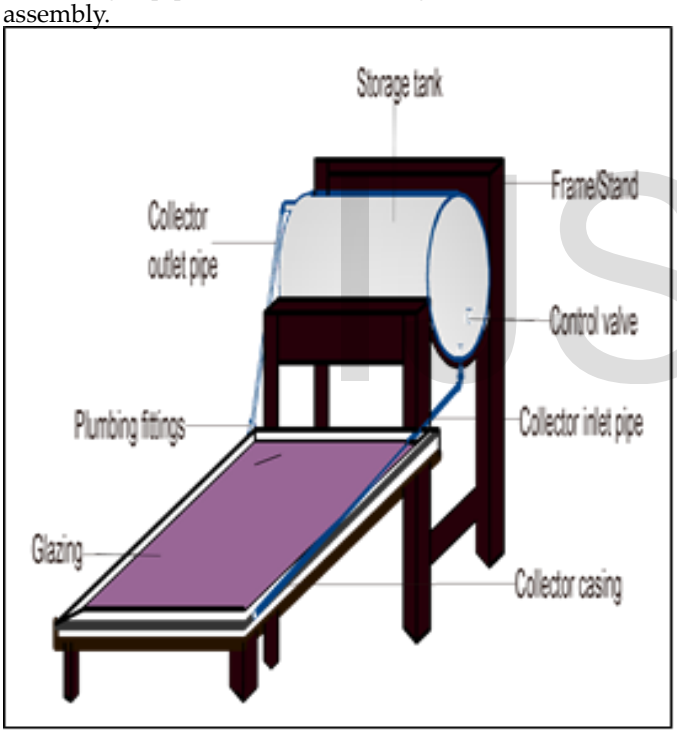

Figure 1: Sketch of the solar water heater with double glazing

3.0 SYSTEM DESIGN

3.1 System Design Equations

3.1.1 Collector useful energy: The useful energy output of a collector with area, A_C, is the difference between the absorbed solar radiation and the thermal loss as expressed by [6] as:

$$Q_u = A_C[S - U_L(T_{pm} - T_a)]^+ \quad (1)$$

The useful energy can also be defined as the quantity of heat required to raise the temperature of the fluid from inlet temperature, T_{in}, to the desired outlet temperature, T_{out}, as given by [5] as:

$$Q_u = mc_p(T_{out} - T_{in}) \quad (2)$$

3.12 Collector area: Combining equations (1) and (2), the collector area, A_C, can be solved for as given by [6] as:

$$A_C = \frac{mc_p(T_{out}-T_{in})}{[S-U_L(T_{pm}-T_a)]^+} \quad (3)$$

3.1.3 Collector mean plate temperature: The mean absorber plate temperature, T_{pm}, usually evaluated in an iterative manner [6] as:

$$T_{pm} = T_{in} + \frac{Q_u/A_C}{F_R U_L}(1 - F_R) \quad (4)$$

[6] developed an expression for estimating T_p, and equated same to be used as T_{pm} as given by [5] as:

$$T_p = T_{in} + 10\ ^\circ\text{C} = T_{pm} \quad (5)$$

3.1.4 Top heat loss coefficient:

An appropriate relation for collector top loss coefficient (U_{top}) as developed by [7] is:

$$U_{top} = \left(\frac{1}{h_{pg_1}+h_{r,pg_1}} + \frac{1}{h_{g_2g_1}+h_{r,g_2g_1}} + \frac{1}{h_w+h_{r,g_2a}} + \frac{L_1}{k_{g_1}} + \frac{L_2}{k_{g_2}}\right)^{-1}, \quad (6)$$

Where;

$$h_w = 2.8 + 3.0V_w \quad (6i)$$

$$h_{g_2g_1} = N_u\frac{k_{g_2}k_{g_1}}{L_2} \quad (6ii)$$

$$N_u = 1 + 1.44\left[1 - \frac{1708}{cos\beta.R_a}\right]\left[1 - \frac{sin(1.8\beta)^{1.6}\times 1708}{cos\beta.R_a}\right] + \left[\left(\frac{cos\beta\times R_a}{5830}\right)^{1/3} - \quad (6iii)$$

$$h_{pg_1} = N_u\frac{k_pk_{g_1}}{L_1} \quad (6iv)$$

$$R_a = \frac{1}{T_{pm}} \times \frac{g\times T_{pm}-T_{g_1}(L_1)^3}{\nu\alpha} \quad (6v)$$

$$T_p = T_{in} + 10\ ^\circ\text{C} = T_{pm} \quad (6vi)$$

$$h_{r,pg_1} = \frac{\sigma.(T_{pm}^2+T_{g_1}^2).(T_{pm}+T_{g_1})}{\varepsilon_p^{-1}+\varepsilon_{g_1}^{-1}-1}, \quad (6vii)$$

$$T_{g_1} = T_a \quad (6viii)$$

$$T_{g_2} = \frac{\left[12\times10^{-8}(T_a+0.2T_p)^3+h_w\right]^{-1}+0.3L_2}{\left[6\times10^{-8}(\varepsilon_p+0.028)(T_p+0.5T_a)^3+0.6L_{pg}^{-0.2}\{(T_p-T_a)cos\beta\}^{0.25}\right]^{-1}} \quad (6ix)$$

$$h_{r,g_2g_1} = \frac{\sigma.(T_{g_2}^2+T_{g_1}^2).(T_{g_2}+T_{g_1})}{\varepsilon_{g_2}^{-1}+\varepsilon_{g_1}^{-1}-1}, \quad (6x)$$

$$h_{r,g_2a} = \varepsilon_{g_2}.\sigma.(T_{g_2}^2+T_s^2).(T_{g_2}+T_s) \text{ and} \quad (6xi)$$

$$T_s = 0.0552(T_a)^{1.5} \quad (6xii)$$

3.1.5 Collector heat removal factor (F_R):

The collector heat removal factor, F_R, is the ratio of the useful energy gain of the collector to the useful energy gain if the whole collector surface were at the fluid inlet temperature. F_R can be expressed as [6]:

$$F_R = \frac{\dot{m}C_p}{A_C U_L}\left[1 - exp\left(-\frac{A_C U_L F'}{\dot{m}C_p}\right)\right] \quad (7)$$

where;

$$F' = \frac{1/U_L}{W\left[\frac{1}{U_L[D_i+(W-d_i)F]}+\frac{1}{C_b}+\frac{1}{\pi D_i h_{f_i}}\right]} \quad (7i)$$

$$F = \frac{tanh\left[\frac{m(W-d_i)}{2}\right]}{\frac{m(W-d_i)}{2}} \quad (7ii)$$

and;

$$m = \sqrt{\frac{U_L}{k\delta}} \quad (7iii)$$

3.1.6 Solar fraction ($S.F.$):

This is the fraction of the total hot water energy that is supplied by the solar water heater and can be calculated using [8]:

$$S.F. = \frac{Q_s - Q_{aux}}{Q_s} \quad (8)$$

3.1.7 System efficiency (η_c):

The efficiency of the solar collector can be determined through a number of ways. One of such ways is the Hottel – Whillier equation which defines the efficiency in terms of the collector heat removal factor (F_R), given in equation (7) by [5]:

$$\eta_c = \frac{F_R[S - U_L(T_{pm} - T_a)]^+}{H_T} \quad (9)$$

3.2 Design Analysis

The solar water heater is divided into the following three major components namely: collector assembly (including glazing, absorber plate, fluid passage tubes and casing), storage tank and stand (frame). Zaria is located between latitude 11°11′ and 11°13′ North, and between longitude 7°30′ and 7°45′ East of the Greenwich meridian. It belongs to the tropical continental type of climate, it has two distinct seasons: the dry or harmattan season (October to March) and wet season (April to September). Mean monthly temperature is about 30 °C [13 and 11]. The water heater was designed to suit the weather and climatic conditions of Zaria.

3.2.1 Solar resources and weather data for Zaria:

Solar radiation and meteorological data (maximum temperature, ambient temperature, minimum temperature and wind velocity etc.) are two very important driving functions for any solar system design and they often seem to be highly random and irregular. Two types of solar radiation data are widely available; first is monthly average daily total radiation on a horizontal surface, $\overline{H}$ and the second is hourly total radiation on a horizontal surface, I, for each hour for extended periods such as one or more years [6]. The monthly average daily Meteorological data for Zaria was generated from weather data processor of TRNSYS 16 software and was used for the design analysis and simulation of the solar water heater.

3.2.2 System design assumptions:

A number of simplifying assumptions were made in order to model the design without obscuring the basic physical situation. These assumptions are as follows [6]:

i. Performance and operation of the solar water heater assembly is in a steady state.
ii. Fluid flow inside the tubes is laminar and uniformly distributed.
iii. Temperature drop through the glazing (covers) is negligible.
iv. Temperature gradient through the absorber plate is negligible.
v. Temperature gradient around the fluid passage tubes is negligible.
vi. Effect of dust and dirt on the collector glazing are negligible.

3.2.3 Design considerations:

The solar water heater design took into cognizance the following important design parameters:

i. The mean daily solar irradiation (insolation) and the mean daily heat load (requirement) was used to determine the design month.
ii. Design load for the system was assumed to be constant for all the months (January to December).
iii. Desired water outlet temperature, T_{out}, (70 °C).
iv. Volume of water to be heated (100 L or 0.1 m^3)
v. Collector tilt angle (β): The collector will be tilted to an angle equivalent to $\pm$ 1° of the latitude of the location (Zaria) according to [12].

3.3 System Design Approach

Performance and reliability of a solar water heater requires proper sizing of its components as well as accurate prediction of the system's performance (delivered useful energy and outlet temperature; solar fraction and thermal efficiency etc.). It is therefore, of paramount importance to properly size the system components; as well as determine system characteristics through calculation of system design parameters.

3.3.1 Determination of design parameters:

The system design parameters and characteristics established based on equations (1) to (9) were numerically evaluated using programme codes developed in MATLAB (2013) programming language. Monthly average daily solar radiations, ambient temperature and wind speed for Zaria were generated from weather data processor of TRNSYS 16 software and used as input data for the calculations. The meteorological data (monthly average daily radiations, ambient temperature and wind speed) for Zaria, Nigeria are shown in Table 1.

Table 1 Meteorological data for location (Zaria)

MONTH	Recommended days(n)	$\bar{H}$ (MJ/s.m^2.day)	$\bar{H}_T$ (MJ/s.m^2.day)	$\bar{H}_b$ (MJ/s.m^2.day)	T_a (^{0}C)	$\bar{V}_W$ (m/s)
JANUARY	17	2.26	2.53	2.06	26.0	2.20
FEBRUARY	47	2.50	2.70	2.20	29.0	3.00
MARCH	75	2.62	2.70	2.12	32.3	1.90
APRIL	105	2.49	2.45	1.69	36.0	3.15
MAY	135	2.05	1.96	1.17	34.0	2.05
JUNE	162	2.01	1.89	1.08	27.4	3.10
JULY	198	1.81	1.72	9.25	31.5	2.10
AUGUST	228	1.70	1.66	7.94	25.5	2.15
SEPTEMBER	258	1.95	1.98	1.14	27.0	2.60
OCTOBER	288	2.19	2.32	1.59	29.8	2.40
NOVEMBER	318	2.29	2.54	2.00	27.2	1.95
DECEMBER	344	2.17	2.45	1.95	27.6	2.50
AVERAGE		2.17	2.24	1.56	29.0	2.00

Source: Type 9 weather data processor of TRNSYS 16 software (2017)

3.3.2 *Determination of design month:*

In determining the design month, it is important to note one key variable known as the clearness index (K_T) defined as ratio of the monthly average daily radiation on a horizontal surface to the monthly average daily extra-terrestrial radiation. Simply put, the month with lowest clearness index is considered the design month.

The clearness index, K_T, is mathematically defined as:

$$K_T = \frac{\bar{H}}{\bar{H}_o} \tag{10}$$

The design load was earlier assumed to be constant throughout the year, therefore, the design month was considered to be the month with the least solar radiation. Calculations of the system design parameters and subsequent components sizing was done based on the design month's average daily solar radiation and weather data for Zaria.

3.4 Design Parameters Optimisation and System Model Simulation:

The design parameters optimisation procedure was done in two parts. The first was done to study the effects and sensitivity of varying selected design parameters on the objective functions in order to determine the proper system characteristics that satisfy performance. Solar radiations, ambient temperature, fluid inlet and outlet temperatures, wind speed and monthly average daily system characteristics for the design month were used as input data into the programme codes written in MATLAB programming language. These programme codes were used to study the effects of varying some selected system characteristics (air gap space, fluid passage tube diameters and absorber plate thickness) on the chosen system design objective functions which are collector heat removal factor, F_R and top heat loss coefficient, U_{top}.

The second part of the optimisation was conducted using TRNSYS 16 software to simulate and predict the system performance using different system component sizes. The software used has the ability to graphically visualise the effect of varying components sizes on the system objective functions. The set of components sizes and system design parameters, which met the system design load (load temperature) after simulation were chosen as the final adopted system design components sizes.

3.4.1 *System performance simulation:*

The system performance was numerically simulated using weather data based on Typical Meteorological Year (TMY) in TRNSYS 16 software for Zaria with the system characteristics as presented in Tables 2 and 3. The system schematic model used for the simulation is as shown in Figure 2. Results of the simulation are presented in section 4.

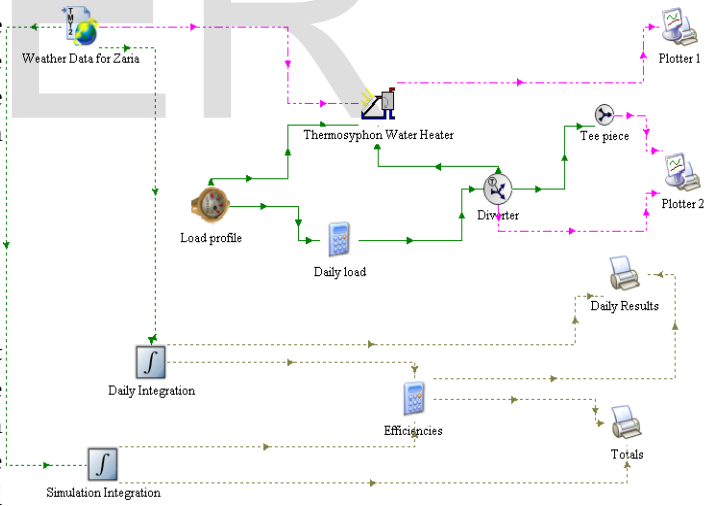

Figure 2: Schematic model of the water heater in TRNSYS 16 simulation studio

3.4.2 *Validation of Simulation Model:*

The water temperature in the storage tank and collector and the solar radiation measured during the experiment were used as validation parameters to validate the predicted system performance obtained from the model. These temperatures were chosen because they serve as important parameters to both the designer and the end user. Storage tank and collector water temperatures and solar radiation were measured at an interval of

one hour starting from 8:00 am to 5:00 pm daily for a period of 3 days and the results were recorded. No water was taken from the storage tank during the process of testing; this was to facilitate the experimentation.

The Nash-Sutcliffe coefficient of Efficiency (NSE) statistical method was employed to validate the predictive power of the model. This method was considered to be objective and provided unbiased indication of the model's predictive power [9]. The Nash-Sutcliffe coefficient of Efficiency is defined as follows:

$$NSE = 1 - \frac{\sum_{i=1}^{n}(X_{model,i} - X_{obs,i})^2}{\sum_{i=1}^{n}(X_{model,i} - \bar{X}_{obs})^2} \quad (11)$$

Nash-Sutcliffe efficiencies can range from -∞ to 1. An efficiency of 1 (NSE = 1) corresponds to a perfect match between model and observations. An efficiency of 0 indicates that the model predictions are as accurate as the mean of the observed data, while an efficiency less than zero (-∞<E<0) occurs when the observed mean serves as a better predictor than the model [10].

4.0 RESULTS AND DISCUSSION

The results of calculations of R_b, monthly average ratio of beam radiation on a tilted to horizontal surface; $\bar{H}_o$, monthly average extra-terrestrial daily radiation on a horizontal surface; $\bar{H}_d$, monthly average total diffused radiation on horizontal surface; δ, declination; $\bar{\omega}_s$, monthly average sunset hour angle; $\bar{H}$, monthly average daily radiation on a horizontal surface and K_T, monthly average clearness index, are shown in Table 2. From Table 2, it can be seen that the value of the clearness index, $\bar{K}_T$, is above 0.65 for the months of January, February, March, April, October, November and December. This goes to show that for these months, over 65 % of the sun's extraterrestrial radiation, $\bar{H}_o$, is received on a horizontal surface at the location under consideration (Zaria). The values of $\bar{K}_T$, decreased to values lower than 0.65 between the months of May and September; with the least value of 0.4675 in August. August is therefore, chosen as the design month. This value of $\bar{K}_T$, for the month of August showed that the least amount of solar energy received in the location under consideration (Zaria) is in the month of August. The annual average value of $\bar{K}_T$, for the location under consideration (Zaria) is **0.6248** which is a good solar potential for design of any kind of solar system. The variations in the average values of $\bar{K}_T$, can be attributed to the amount of cloud cover in the sky for all the months in question.

Table 2 Simulated monthly solar data for Zaria

MONTH	R_b	$\bar{H}_o$ (MJ/s.m².day)	$\bar{H}_d$ (kJ/s.m².day)	δ (°)	$\bar{\omega}_s$ (°)	$\bar{H}$ (MJ/s.m².day)	$\bar{K}_T$
JAN	1.1578	3.24	200	-20.9170	14.0388	2.26	0.6986
FEB	1.0741	3.33	300	-12.9546	13.5288	2.50	0.7503
MAR	0.9871	3.46	500	-02.4177	13.3866	2.62	0.7562
APR	0.9397	3.61	800	09.4149	13.8137	2.49	0.6892
MAY	0.9187	3.77	880	18.7919	14.7871	2.05	0.5435
JUNE	0.9156	3.89	930	23.0859	15.5903	2.01	0.5171
JULY	0.9098	3.81	885	21.1837	15.1940	1.81	0.4749
AUG	**0.9612**	**3.64**	**906**	**13.4550**	**14.1386**	**1.70**	**0.4675**
SEPT	1.0008	3.48	810	12.2169	13.4757	1.95	0.5602
OCT	1.0186	3.34	600	-9.5994	13.4286	2.19	0.6557
NOV	1.1075	3.24	290	-18.9120	13.8664	2.29	0.7075
DEC	1.1426	3.21	220	-23.0496	14.2646	2.17	0.6771
AVE.	**1.0111**	**3.50**	**610**		**14.1261**	**2.17**	**0.6248**

4.2.1 *Air gap spacing optimisation:*

The results of varying the air – gaps L_1 and L_2 and the resultant effect on the top heat loss coefficient, U_{top} are presented in Figure 3.

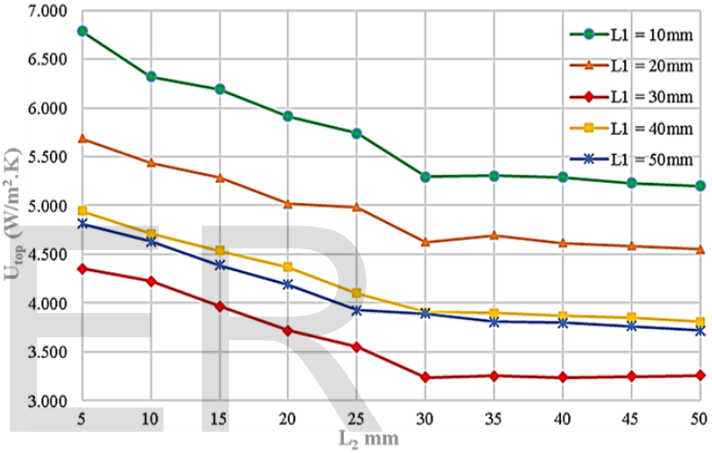

Figure 3: Variation of air – gap spacing $L_1 and\ L_2$ on top heat loss coefficient (U_{top})

Figure 3 shows the result of varying the air gap spaces (L_1 and L_2) on the top heat loss coefficient, U_{top}. It can be observed that U_{top} has the highest value of 6.785 *W/m².K* for a combination of air – gaps (L_1 = 10 mm and L_2 = 5 mm). L_1 was maintained at 10 mm, while L_2 was again varied between 10 mm to 30 mm which showed a slight decrease in U_{top} from 6.785 *W/m².K* to 5.293 *W/m².K* which represents a percentage decrease of 21.99 %. As L_2 was further increased from 30 mm to 50 mm, there was no further significant decrease in U_{top} as seen from the Figure (5.293 *W/m².K* to 5.198 *W/m².K* which represents only 1.79 % decrease). This trend continued for values of L_1 = 20 mm, 30 mm, 40 mm and 50 mm respectively and in each case, L_2 was varied between 5 mm to 50 mm respectively. Since there was no significant decrease in the values of U_{top} for all cases of L_1 beyond 30 mm, it can therefore be deduced that the combination of L_1 and L_2 with the possible minimum heat loss to the surface can be taken for values of both L_1 and L_2 between 30 mm to 50 mm. This research however, adopted a combination of L_1 = L_2 = 30 mm because L_2 also had its least value of U_{top} = 3.241 *W/m².K* at 30 mm.

4.2.2 Collector tube diameter (risers and headers) optimisation:

The effect of varying the riser tubes internal diameter (d_i) on the collector heat removal factor, F_R, over a range of header tubes internal diameters, D_i (0.015 m, 0.020 m, 0.025 m, and 0.030 m), while keeping the collector heat loss coefficient, U_L (4.93 W/m^2K), collector area, A_C (2.5 m^2), tube centre to centre distance, W (0.010 m) and plate thickness (0.006 m) constant is shown in Figure 4.

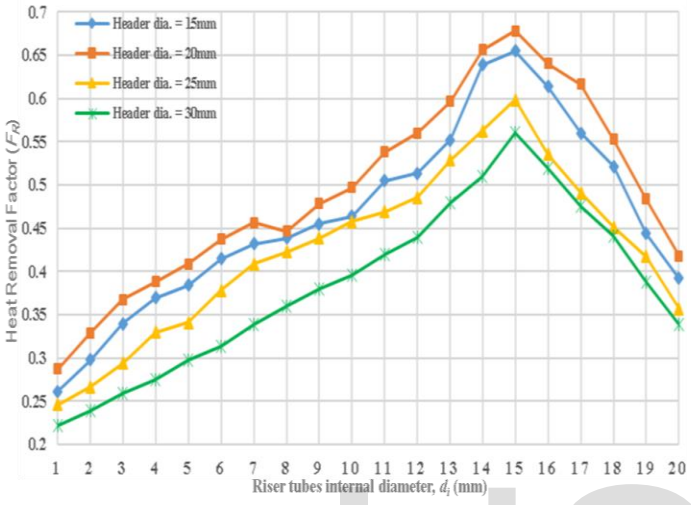

Figure 4: Variation of riser tubes internal diameters (d_i) on heat removal factor (F_R) for a range of header tubes internal diameters (D_i).

Figure 4 shows that as d_i increased from 1 to 15 mm, heat removal factor, F_R, for a header tube diameter, D_i of 20 mm increased from 0.2871 to 0.6783 which represents an increased percentage of 57.67 %. However, as d_i was further increased from 15 mm to 20 mm with the header diameter maintained at 20 mm, the heat removal factor, F_R, began to decrease from 0.6783 to 0.4179 which represents a percentage decrease of 38.39 %. This trend was also observed for header diameters of 15 mm, 25 mm and 30 mm respectively as seen from the graph. Since, the value of the heat removal factor has a direct relationship with the thermal efficiency of the system, a combination of header diameter of 20 mm and riser diameter of 15 mm gave the highest value of the heat removal factor of 0.6783. Therefore, these values were considered suitable for the system optimum performance and as such were selected for the design.

4.2.3 Absorber plate thickness optimisation:

The result of varying the absorber plate thickness on the collector heat removal factor for same collector characteristics are presented in Figure 5.

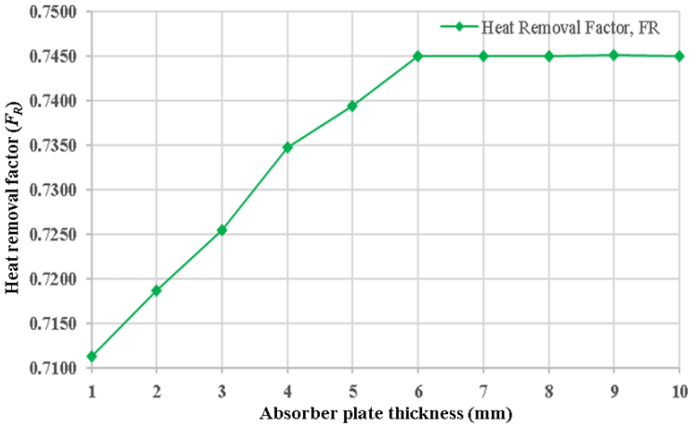

Figure 5: Variation of collector absorber plate thickness on heat removal factor (F_R) for a given range of collector characteristics.

Figure 5 shows an increase in the value of the heat removal factor, F_R, from 0.7113 to 0.7449 as the plate thickness was varied from 1 – 6 mm which represents a percentage increase of about 3.36 %. Again, as the plate thickness was varied from 6 mm to 10 mm, the heat removal factor, F_R, did not show any significant increase or decrease in value. This shows that any plate (of specified material) of thickness equal to 6 mm and above may not significantly affect the performance of the system, once all other parameters are as required. Therefore, in order to cut down system cost and at the same time maintain system desired performance, commercially available absorber plate of size 6 mm thick (Aluminium plate) was selected for the design.

4.3 System design parameters and characteristics:

Table 3 and Table 4 show the final system characteristics and design parameters selected for the system performance simulation using TRNSYS 16 software.

Table 3: System characteristics

Description	Value/Type
Total aperture area	2.500 m^2
Tank diameter	0.480 m
Storage tank capacity	100 *litres*
Riser tubes material	Copper
Number of riser tubes	12
Absorber plate thickness	0.006 m
Internal tube diameter (risers)	0.015 m
External tube diameter (headers)	0.020 m
Thermal conductivity of insulation material	0.080 W/mK
Thermal conductivity of absorber plate material	225 W/mK
Insulation thickness	0.050 m
Absorber surface	painted matt black
Glass type	4 mm low iron glass
Collector insulation	fibre glass wool 50 mm thick (sides and back)

L_i	Collector inlet pipe length (m)	1.500
NB_1	Number of right angle bends in inlet pipe	2
NB_2	Number of right angle bends in outlet pipe	2
V_t	Tank volume (m^3)	0.150
H_t	Tank height (if vertical) or length (if horizontal) (m)	0.900
H_R	Height of collector return to tank above bottom of tank (m)	0.480

Table 4: System final adopted design parameters and components sizes

Parameter	Description	Value/ Type
A_C	Collector area (m^2)	2.500
$F_R(\tau\alpha)_n$	Intercept of efficiency vs. (Ti-Ta)/IT curve	0.770
$F_R U_L$	Negative of slope efficiency vs. (Ti-Ta)/IT ($kJ/hm^2{}^\circ C$)	4.700
β	Collector slope (*degrees*)	12
N_R	Number of parallel collector risers	12
d_R	Riser diameter (m)	0.015
d_H	Header diameter (m)	0.020
l_H	Header length (m)	1.300
h_c	Vertical distance between collector outlet and inlet (m)	0.330
h_o	Vertical distance between outlet of tank and inlet of collector (m)	0.390
d_i	Collector inlet tube diameter (m)	0.025
d_o	Collector outlet tube diameter (m)	0.025
L_o	Collector outlet pipe length (m)	0.350
L_i	Collector inlet pipe length (m)	1.500
NB_1	Number of right-angle bends in inlet pipe	2
NB_2	Number of right-angle bends in outlet pipe	2
V_t	Tank volume (m^3)	0.150
H_t	Tank height (if vertical) or length (if horizontal) (m)	0.900
H_R	Height of collector return to tank above bottom of tank (m)	0.480

4.4 Comparison of Simulated Results with Experimented Results:

The experimented (measured) hourly solar radiation, ambient temperature, tank inlet temperature and collector inlet temperatures were all compared with their simulated (predicted) counterparts from the model (Type 109 weather data processor of TRNSYS 16 software) and the results of these comparisons are shown in Figures 5 to 7.

Figure 5 shows that the model slightly over estimated the hourly solar radiation for most parts of the day for the location under consideration (Zaria) on November 10, 2016. However, the computed Nash-Sutcliffe coefficient of Efficiency (NSE) value of 0.8886 between the measured (experimented) solar radiation and the simulated solar radiation indicated that the error was little and that the model was 88.86 % accurate in predicting the actual solar radiation on November 10, 2016. The simulated and experimented solar radiations recorded on November 11, 2016 and November 12, 2016 respectively follow the same trend as presented in Figures 6 and 7 respectively with the simulated hourly solar radiations being slightly higher than the experimented hourly solar radiations.

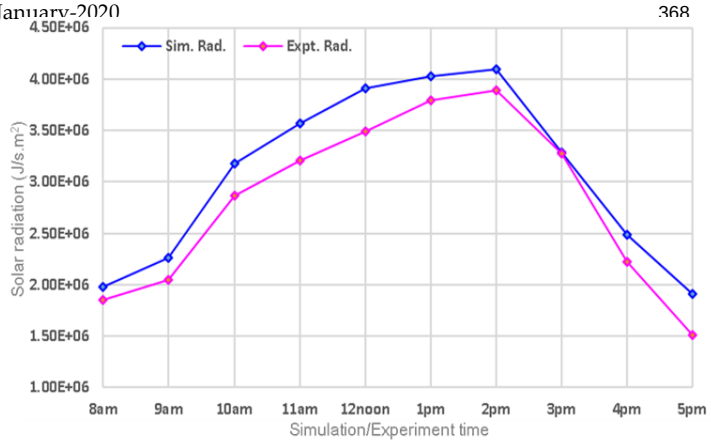

Figure 5: Comparison of hourly solar radiation of Zaria recorded during experiment with values obtained from simulation on November 10, 2016

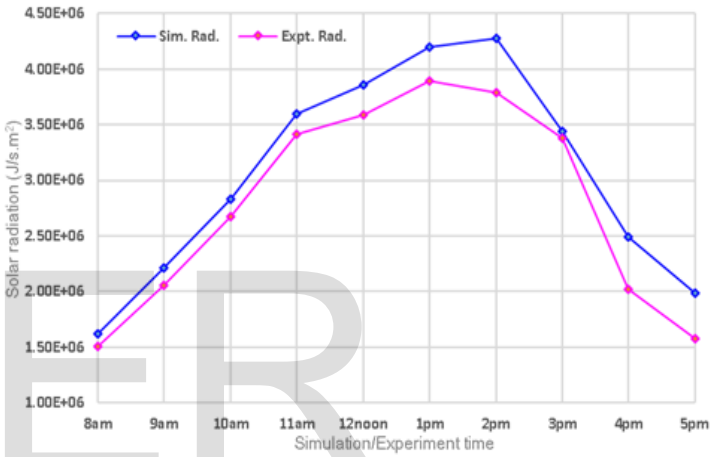

Figure 6: Comparison of hourly solar radiation of Zaria recorded during experiment with values obtained from simulation using TRNSYS 16 software on November 11, 2016.

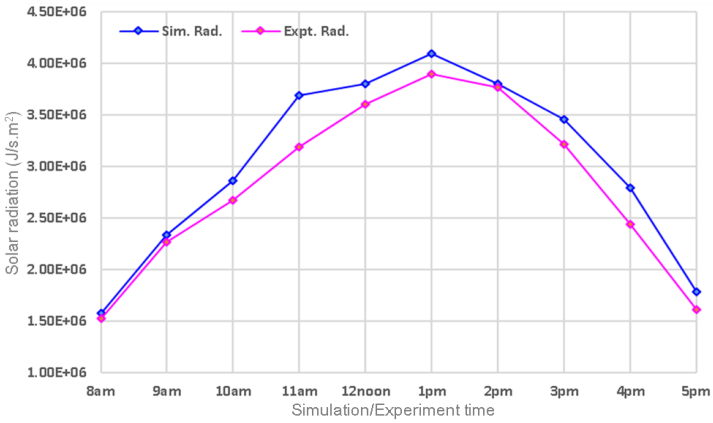

Figure 7: Comparison of hourly solar radiation of Zaria recorded during experiment with values obtained from simulation using TRNSYS 16 software on November 12, 2016.

The variation of the storage tank and collector hourly inlet temperatures recorded during the experiment in comparison with the simulated ones for November 10, 2016 are presented in Figure 8. Figure 8 shows an increase in the experimented tank

inlet temperature from an initial value of 33 ℃ at the start of the experiment at 8:00 am reaching its peak value of 100 ℃ at 2:00 pm. This temperature started to decrease after 3:00 pm to a value of 66 ℃ at the end of the experiment at 5:00 pm. The variation in hourly collector inlet temperature also followed the same trend, with maximum value of 72 ℃ recorded at 2:00 pm.

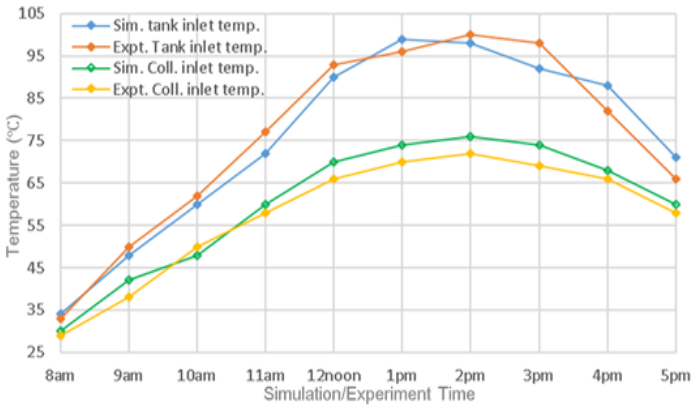

Figure 8: Comparison of experimented hourly inlet temperatures of storage tank and collector with simulated values for November 10, 2016.

4.5 Analysis of the Predictive Power of the TRNSYS 16 Simulation Software:

Table 5 shows the summary of the results of statistical analysis (NSE) used to analyse the predictive ability of the system model (TRNSYS 16 software) based on the simulated and experimented hourly solar radiation, storage tank inlet temperatures and collector inlet temperatures for November 10, 2016 to November 12, 2016.

Table 4.7: Results of statistical analysis (NSE)

DESCRIPTION	NSE
Solar radiation for November 10, 2016	0.8886
Storage tank inlet temperature for November 10, 2016	0.9656
Collector inlet temperature for November 10, 2016	0.9528
Solar radiation for November 11, 2016	0.8983
Storage tank inlet temperature for November 11, 2016	0.9763
Collector inlet temperature for November 11, 2016	0.9335
Solar radiation for November 12, 2016	0.9230
Storage tank inlet temperature for November 12, 2016	0.9749
Collector inlet temperature for November 12, 2016	0.9426

Table 5 shows an NSE value of 0.8886 between the simulated and experimented hourly solar radiations for November 10, 2016. This NSE value of 0.8886 indicates that the model was able to predict the hourly solar radiations with 88.86 % degree of accuracy. Table 5 also shows an NSE value of 0.9656 between the simulated and experimented results. This NSE value of 0.9656 indicates that the model was able to predict the hourly storage tank inlet temperature with 96.56 % degree of accuracy. This also implies acceptable quality of fit between the experimented data and the simulated data since, the closer the NSE value is to 1 (one), the better the predictive power of the model [9]. An NSE value of 0.9528 between the simulated and experimented collector inlet temperatures on November 10, 2016 was also presented. This also shows that the model was able to predict the hourly collector inlet temperatures with 95.28 % degree of accuracy.

5.0 CONCLUSION

A solar water heater designed and optimised based on weather data for Zaria, (latitude 11.12 °N and longitude 7.8 °E), hot water storage capacity of 0.1m^3 and desired water outlet temperature of 70 ℃ at the department of Mechanical Engineering, Ahmadu Bello University, Zaria, Nigeria. The results of this research had led to the following conclusions:

1. The parametric study (optimisation) carried out on some selected system components (air – gap space, collector tube diameters and absorber plate thickness) revealed that the design objective functions (heat removal factor, F_R, and top heat loss coefficient, U_{top}) were affected in the following ways:
   a. The top heat loss coefficient, U_{top}, decreased as both the lower (L_1) and the upper (L_2) air – gaps were varied from 5 mm to 50 mm until a combination of L_1 and L_2 ($L_1 = L_2 = 30\ mm$) which gave the least top heat loss coefficient of 3.241 $W/m^2.K$ was achieved. It was therefore, concluded that for the system to have a possible minimum heat loss to the surface, a combination of lower and upper air – gaps ($L_1 = L_2 = 30\ mm$) was adopted.
   b. Varying the collector tube internal diameters (for risers and headers) also had effect on the heat removal factor, F_R. As the riser diameters were increased from 1 to 15 mm, there was noticeable increase in the value of F_R, from 0.2615 to 0.6548 (about 60.1 %) while maintaining the header diameter at 20 mm. However, increasing the riser diameter 16 to 20 mm and still maintaining the header diameter at 20 mm reveals a decrease in the value of F_R from 0.6136 to 0.3917 (about 36.16 %). It was concluded from the study that, system optimum performance was achieved with a combination of riser diameter of 15 mm and header diameter of 20 mm.
   c. The heat removal factor F_R, increased from 0.7113 to 0.7449 (about 4.51 %) as the plate thickness was varied from 1 to 6 mm. However, increasing the plate thick-

ness beyond 6 mm, showed no significant change in the value of F_R, which led to the conclusion that optimum system performance coupled with the least cost of absorber can be achieved with an absorber plate of thickness 6 mm of specified material (Aluminium).

2. Hourly simulated and experimented system efficiencies were studied for the three (3) days in which the experiment was conducted and they followed similar trends with the simulated system efficiencies being higher than the experimented efficiencies from start (8:00 am) to the end of the experiment around 5:00 pm for the three (3) days. The average daily simulated/experimented efficiencies for the three (3) days were 60 %/58 %, 59 %/56 % and 56 %/53 % respectively. This difference in performance can be largely attributed to the fact that the data used for the simulation were strictly based on assumptions while the actual/measured data were used for the experiments.

6.0 ACKNOWLEDGMENT

My sincere gratitude goes to God Almighty for giving me the privilege to successfully carry out this research work and I acknowledge His love, grace and mercies upon my life throughout the entire period of this exercise. I would also like to extend my profound gratitude to my supervisors; Prof. G.Y. Pam and Engr. Dr. F.O. Anafi, for their candid advice and guidance from the very early stage of this research work as well as giving me all the necessary assistance throughout the duration of the work. I am also indebted to my family members for their love, encouragement, support (both in cash and kind), prayers and selfless sacrifices to see to the completion of this work. I lack words to express how much I feel, knowing fully well that I don't even deserve the love you all have shown me. God bless you real and I pray that we keep this bond of love strengthened as we continue to stand in the gap for each other. To my PEARL (my wife), as I love to call her, thank you for your understanding, patience, care and above all your sacrificial love. I just can't express how much I appreciate you and for been there for me at all times. You've encouraged and supported me right from the very beginning up to the very end. You are truly a darling. Finally, this work would not have been successful without the guidance, encouragement and support of several individuals (too numerous to mention), who in one way or another contributed and extended their valuable assistance in the preparation and completion of this work. I appreciate you all and I pray our good Lord bless and reward you all. Thank You!

7.0 REFERENCES

[1] British Petroleum (2014). Renewable Energy, viewed 28 April 2014, <http://www.bp.com/sectiongenericarticle.do?categoryId=9023767&contentId=7044196>.

[2] Chakravarty S., Chikkatur A., de Coninck H., Pacala S., Socolow R., and Tavoni M. (2014). 'Sharing Global CO2 Emission Reductions among One Billion High Emitters', Proceedings of the National Academy of Sciences, 106, (29): 84–88.

[3] Mossad R. (2006). 'Numerical Simulation to Optimise the Design of Double Glazed Doors for Closed Refrigerated Vertical Display Cabinets', 13th International Heat Transfer Conference IHTC–13, Redding, CT, USA, 2(4): 88-94.

[4] Marwaan A.H. AL-Khaffajy and Mossad R. (2013). 'Numerical Evaluation of the Performance of an Indirect Heating Integrated Collector Storage Solar Water heater', 9th Australasian Heat and Mass Transfer Conference (9AHMTC) Monash University, Melbourne, Victoria, Australia, 9 (1): 117–122.

[5] Zwalnan S.J. (2015). Design, Simulation, Construction and Performance Evaluation of a Thermosyphon Solar Water Heater (Master's Dissertation, Department of Mechanical Engineering, Ahmadu Bello University, Zaria).

[6] Duffie J.A and Beckman W.A. (2013). 'Solar Engineering of Thermal Processes', Fourth Edition, John Wiley & Sons Inc., Hoboken New Jersey. 4: 156 – 189, 477 – 509.

[7] Subiantoro A. and Ooi K. T. (2013). 'Analytical models for the computation and optimisation of single and double glazing flat plate solar collectors with normal and small air gap spacing.' Journal of Applied Energy, 104 (1):392–399 http://dx.doi.org/10.1016/j.apenergy.2012.11.009

[8] Buckles, W.E., and Klein, S.A. (1980). 'Analysis of solar domestic hot water heaters' Solar Energy, 25 (5): 417–424. Julien, G. A, Emmanuel, L., Clément, A., Rufin, O. A., and Brice, A. S. (2013). Modeling solar energy transfer through roof material in Africa Sub-Saharan Regions. ISRN Renewable Energy, 34 (7): 632–645.

[9] Julien, G. A, Emmanuel, L., Clément, A., Rufin, O. A., and Brice, A. S. (2013). Modeling solar energy transfer through roof material in Africa Sub-Saharan Regions. ISRN Renewable Energy, 34 (7): 632–645.

[10] Neil, J. S. (2010). Encyclopedia of Research Design. Online ISBN: 9781412961288 Publisher: SAGE Publications, Inc.

[11] Mohammed B. A., Ismail I. R., Mohammed H. I., Mahmoud M. G., and Mohammed K. H., (2015). 'Design, Construction and Installation of 250 – liter Capacity Solar Water heater at Danjawa Renewable Energy Model Village', Int'l Journal of Engineering Science, 4 (3): 39–44

[12] Rajput R.K. (2012). 'Heat and Mass Transfer'. S. Chand and Company Ltd., Ram Nagar, New Delhi. 5th Revised Edition;10B (314): 14, 142–144

[13] Yusuf B.M. (2011): 'Introduction to Renewable Energy Technologies'. Albarka Printing Press, Birnin kebbi, :50.J.M.P. Martinez, R.B. Llavori, M.J.A. Cabo, and T.B. Pedersen, "Integrating Data Warehouses with Web Data: A Survey," *IEEE Trans. Knowledge and Data Eng.*, preprint, 21 Dec. 2007, doi:10.1109/TKDE.2007.190746.(PrePrint)